Research article

Functional analysis of a frame-shift mutant of the dihydropyridine receptor pore subunit (α_{1S}) expressing two complementary protein fragments

Chris A Ahern, Paola Vallejo, Lindsay Mortenson and Roberto Coronado*

Address: Department of Physiology, University of Wisconsin School of Medicine, Madison, WI 53706, USA

E-mail: Chris A Ahern - cahern@physiology.wisc.edu; Paola Vallejo - paolavallejo@hotmail.com;
Lindsay Mortenson - lindsay@physiology.wisc.edu; Roberto Coronado* - coronado@physiology.wisc.edu

*Corresponding author

Abstract

Background: The L-type Ca^{2+} channel formed by the dihydropyridine receptor (DHPR) of skeletal muscle senses the membrane voltage and opens the ryanodine receptor (RyR1). This channel-to-channel coupling is essential for Ca^{2+} signaling but poorly understood. We characterized a single-base frame-shift mutant of α_{1S}, the pore subunit of the DHPR, that has the unusual ability to function voltage sensor for excitation-contraction (EC) coupling by virtue of expressing two complementary hemi-Ca^{2+} channel fragments.

Results: Functional analysis of cDNA transfected dysgenic myotubes lacking α_{1S} were carried out using voltage-clamp, confocal Ca^{2+} indicator fluoresence, epitope immunofluorescence and immunoblots of expressed proteins. The frame-shift mutant (fs-α_{1S}) expressed the N-terminal half of α_{1S} (M1 to L670) and the C-terminal half starting at M701 separately. The C-terminal fragment was generated by an unexpected restart of translation of the fs-α_{1S} message at M701 and was eliminated by a M701I mutation. Protein-protein complementation between the two fragments produced recovery of skeletal-type EC coupling but not L-type Ca^{2+} current.

Discussion: A premature stop codon in the II-III loop may not necessarily cause a loss of DHPR function due to a restart of translation within the II-III loop, presumably by a mechanism involving leaky ribosomal scanning. In these cases, function is recovered by expression of complementary protein fragments from the same cDNA. DHPR-RyR1 interactions can be achieved via protein-protein complementation between hemi-Ca^{2+} channel proteins, hence an intact II-III loop is not essential for coupling the DHPR voltage sensor to the opening of RyR1 channel.

Background

The dihydropyridine receptor (DHPR) of skeletal muscle consists of α_{1S}, α_2, β_{1a} and γ_1 subunits [1]. The α_1 subunit is a large four-repeat transmembrane protein of ~220 KDa that contains the basic functional elements of the L-type Ca^{2+} channel, including the Ca^{2+} selective pore and S4

"voltage-sensing" transmembrane segments in each of the four internal repeats [2]. β subunits are ~65 kDa cytosolic proteins essential for membrane trafficking, modulation of channel kinetics, and for excitation-contraction (EC) coupling [3,4]. The α_2 subunit is a highly glycosylated ~175 kDa protein formed by two disulfide-linked pep-

tides [5], whereas the γ_1 subunit is a ~32 kDa skeletal muscle-specific protein of four presumptive transmembrane domains with almost unknown function [6,7].

Skeletal muscle cells utilize the voltage sensors formed by the S4 segments to trigger a rapid elevation of cytosolic Ca^{2+}, thus coupling membrane excitation to muscle cell contraction. Subsequent to charge movements in the voltage sensors, a conformational change in the DHPR is transmitted to the ryanodine receptor (RyR1), presumably, via protein-protein interactions [8]. Ultimately, there is a brief opening of the RyR1 channel resulting in the release of Ca^{2+} from the sarcoplasmic reticulum (SR). Numerous observations have lent support to this view, and especially significant are the functional expression studies in dysgenic myotubes lacking α_{1S}. The dysgenic myotube is devoid of L-type Ca^{2+} current, charge movements and EC coupling. All three are restored in the dysgenic myotube by expression of α_{1S}[9–11]. These results corroborated the essential role of α_{1S} in the mechanism of EC coupling of skeletal muscle cells.

The mechanism by which the DHPR signals the RyR1 is poorly understood [12,13]. Domains in the cytoplasmic linker between repeats II and III have been clearly implicated [14–19], and some regions such as Thr671-Lue690 were suggested to trigger RyR1 opening by binding to RyR1 [15]. However, extensive deletions within the II-III linker that eliminate the RyR1 binding region, and other suggested signaling regions in the II-III loop [16], do not entirely eliminate EC coupling [20,21]. Hence additional domains of α_{1S} and/or other DHPR subunits appear to be engaged by the voltage sensor and contribute to an EC coupling signal. In this respect, the contribution of the $\beta1a$ subunit of the DHPR to EC coupling in skeletal muscle cells has been extensively documented [4,22–24].

In the present report, we characterized a frame-shift mutant of α_{1S} that expresses two complementary fragments of α_{1S}. Complementation between the two α_{1S} fragments produced recovery of EC coupling in dysgenic muscle cells lacking α_{1S}. The results suggest the EC coupling voltage sensor of skeletal muscle is modular in function and can be assembled from separate hemi-Ca^{2+} channel fragments.

Results and Discussion
Expression of a frame-shift mutation of α_{1S} in dysgenic myotubes
Primers for the frame-shift mutant, fs-α_{1S}, were originally designed to delete the 20-mer Thr671-Leu690 in the cytosolic loop between repeats II and III of α_{1S} and to generate a full-length α_{1S} carrying this internal deletion. A proofreading error during a PCR reaction resulted in an amplified DNA with the desired deletion but also contain-

ing an additional thymidine following the TTG codon for Leu670 (Fig. 1A). The one-base shift in reading frame introduced a serine at position 671 followed immediately by a stop codon (Fig. 1B). This frame-shift mutation was re-ligated into an otherwise full-length α_{1S}, subcloned into the mammalian expression vector pSG5, and transfected into dysgenic (α_{1S} null) myotubes. Fs-α_{1S} was abundantly expressed in primary dysgenic myotubes in culture (Fig. 1C) and produced the expected truncated α_{1S} protein (Fig 1D). Western blots using N-terminus T7-tagged fs-α_{1S} and T7-tagged full-length α_{1S} showed that the expressed full-length α_{1S} protein migrated with an apparent molecular weight of approximately 185 KDa under reducing conditions. This result is consistent with the mobility of the native purified skeletal muscle α_{1S} subunit [25]. The fs-α_{1S} migrated with a molecular weight of approximately 90 KDa which is entirely consistent with the theoretical molecular weight of the expressed fragment which was 85.6 KDa. Furthermore, 5-fold overloading of the SDS-PAGE gel failed to detect any fragment of a size comparable to full-length α_{1S} (not shown).

Recovery of EC coupling by the frame-shift a_{1S} cDNA
EC coupling was investigated in voltage-clamped myotubes with simultaneous monitoring of intracellular Ca^{2+} using confocal fluorescence of fluo-4 [26]. Controls shown in Fig. 2A indicated that the overwhelming majority of non-transfected dysgenic muotubes (13 of 15 cells) did not produce detectable Ca^{2+} transients (<0.1 $\Delta F/Fo$) or Ca^{2+} currents (<20 pA/cell) in response to depolarization under voltage-clamp. This is shown in the line-scan images of fluo-4 fluorescence in Fig. 2A and the corresponding traces of ICa^{2+} during a 50-ms depolarization to +30 mV and +90 mV delivered at the start of the line scan in the same cell. However, in two cells (2 of 15 cells) we observed Idys, the low-density endogenous Ca^{2+} current previously described in dysgenic myotubes [27,28]. The reason for the low abundance of this current in these cultured myotubes is unknown. Ca^{2+} currents and stimulated fluorescence for one of the cells expressing Idys is shown in Fig. 2B. We observed a peak ICa^{2+} density of approximately 0.8 pA/pF and a barely detectable fluorescence signal which in Fig. 2B is indicated by the arrow in the trace of integrated fluorescence at +30 mV. This small fluorescence signal disappeared entirely at +90 mV, suggesting it might be contributed directly by Idys or might be due to SR Ca^{2+} release induced by Idys. The voltage dependence of the fluorescence signal and ICa^{2+} are compared in Fig. 2C for the two cells expressing Idys and for the vast majority of cells which altogether did not express intracellular Ca^{2+} transients or ICa^{2+}. The maximum fluorescence signal contributed by Idys, when Idys was present, was <0.2 $\Delta F/Fo$ units. Furthermore, the shape of the fluorescence vs. voltage relationship was bell-shaped and a mirror image of the ICa^{2+} vs. voltage curve. These
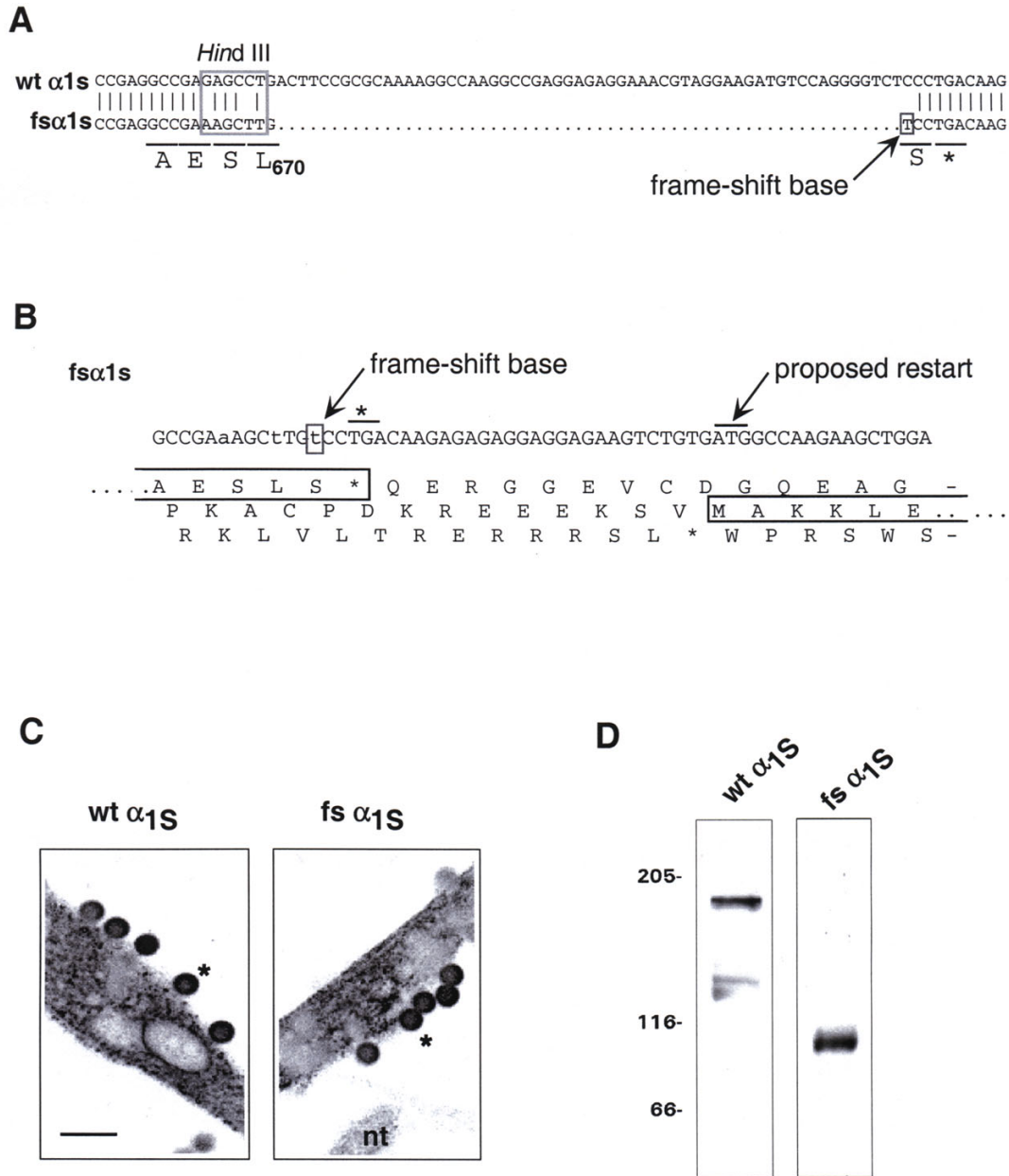
Figure 1
Nucleotide sequence and protein expression of fs-α_{1S}. A) Nucleotide sequence of wt-α_{1S} and fs-α_{1S} in the region of the frame-shift. B) The three reading frames of fs-α_{1S} in the region of the frame-shift are shown. Translation of the C-terminal half of α_{1S} is explained by a restart of translation at the indicated ATG codon which is located 25 bases downstream from the termination codon indicated by the asterisk. C) Confocal images (calibatrion bar is 10 microns) show details of the intracellular distribution of the expressed proteins. Cells were transfected with the CD8 cDNA plus wt-α_{1S} or fs-α_{1S}. Cells were incubated with CD8 antibody beads, fixed, and stained with T7 primary/fluorescein-conjugated secondary antibodies. Pixel intensity was converted to a 16-level inverted gray scale with high-intensity pixels in black color. Asterisks show on-focus CD8 antibody beads (diameter 4.5 microns) bound to cells. NT indicates a non-transfected myotube in the same focal plane of the transfected cell. D) Immunoblots using anti T7 antibody of cultures of dysgenic myotubes expressing wt-α_{1S} and fs-α_{1S}. Indicated are 3 of 7 molecular weight markers run in the same gel.
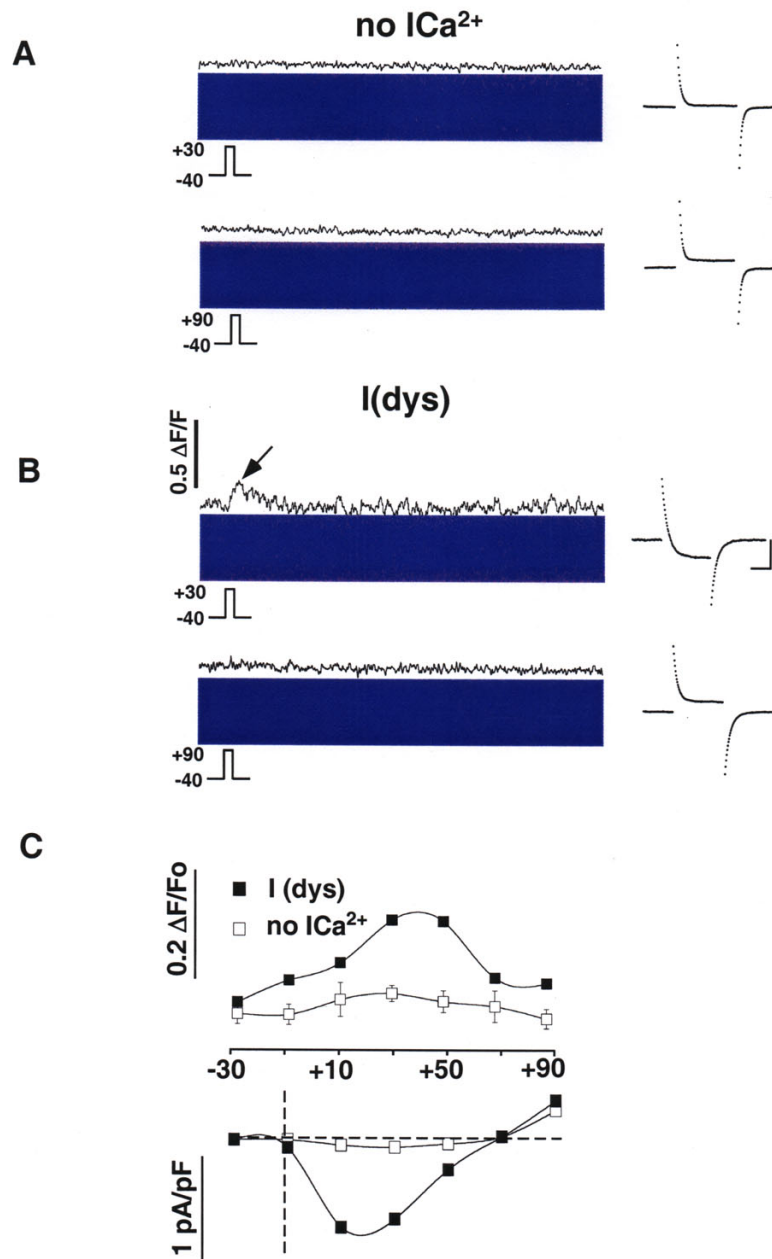
Figure 2
Absence of EC coupling in non-transfected dysgenic myotubes. The confocal line-scan images in color show fluo-4 fluorescence across myotubes in response to a 50-ms depolarization from a holding potential of -40 mV. Line scan images have a constant temporal dimension of 2.05 s (horizontal) and a variable spatial dimension (vertical) depending on the cell size. Traces immediately above each line scan show the time course of the fluorescence change in resting units ($\Delta F/Fo$). The amplitude and the timing of the depolarization are indicated under each line-scan. Arrow indicates a small Ca^{2+} transient elicited in 1 of 2 cells found to express Idys. Traces next to lines-cans show ICa^{2+} during the 50 ms depolarization used to stimulate the Ca^{2+} transient. Current calibration bars are 10 ms and 1 pA/pF. A) Absence of Ca^{2+} transients and ICa^{2+} in a typical dysgenic cell. B) Minor Ca^{2+} transient and ICa^{2+} in a cell expressing Idys. Note that fluorescence calibration bar is 0.5 $\Delta F/Fo$. A 16-color calibration bar in $\Delta F/Fo$ units is included in Fig. 3 for visual reference. C) Voltage dependence of the mean ($\pm$ SEM) ICa^{2+} and mean peak Ca^{2+} transient ($\pm$ SEM) in 13 cells not expressing ICa^{2+} and 2 cells expressing Idys (mean only).
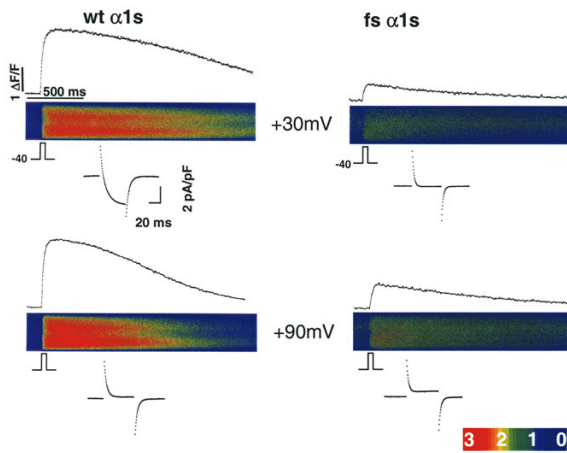
Figure 3
Ca^{2+} transients in dysgenic myotubes transfected with fs-α_{1S}. The confocal line-scan images in color show fluo-4 fluorescence across myotubes in response to a 50-ms depolarization from a holding potential of -40 mV to +30 mV (top) and +90 mV (bottom). Line scan images have a constant temporal dimension of 2.05 s (horizontal) and a variable spatial dimension (vertical) depending on the cell size. Traces immediately above each line scan show the time course of the fluorescence change in resting units ($\Delta F/Fo$). Traces under lines cans show ICa^{2+} during the 50 ms depolarization used to stimulate the Ca^{2+} transient. The amplitude and the timing of the depolarization are indicated under each line scan. Note that fluorescence calibration bar is 1 $\Delta F/Fo$. A 16-color calibration bar in $\Delta F/Fo$ units is included for visual reference.

controls indicated that non-transfected dysgenic myotubes are low-background cells that do not express voltage-activated Ca^{2+} signals of major consequence for the present studies.

Fig. 3 shows that fs-α_{1S} recovered a significant fraction of the voltage-activated Ca^{2+} transient compared to that express by full-length wt-α_{1S}. The magnitude of the fluorescence signal expressed by fs-α_{1S} was approximately 5-fold larger than the largest Ca^{2+} transient detected in non-transfected myotubes expressing Idys, >20-fold larger than the average Ca^{2+} transient detectable in non-transfected cells, and about 1/3 of the maximum SR Ca^{2+} release expressed by the control wt-α_{1S} construct. Thus, we are confident that the voltage-evoked Ca^{2+} transient in cells transfected by fs-α_{1S} cells was a direct consequence of the expressed protein. Also shown in Fig. 3 is ICa^{2+} activated by the 50-ms depolarization used to activate the Ca^{2+} transient. fs-α_{1S} did not express L-type Ca^{2+} current even though it was consistently able to activate the Ca^{2+} transient in 15 of 15 cells. Absence of ICa^{2+} was further verified using longer 500-ms depolarizing pulses (not

shown). The skeletal nature of the EC coupling expressed by fs-α_{1S} is shown in Fig. 4A. The peak Ca^{2+} vs. voltage relationship expressed by fs-α_{1S}, like that of wt-α_{1S}, was sigmoidal in shape reaching a maximum at large positive potentials (>50 mV), a range in which ICa^{2+} is progressively small. The line scans of Fig. 4B further confirmed that a Ca^{2+} transient of similar shape and magnitude was observed in a fs-α_{1S} transfected myotube in the absence of external Ca^{2+}. Hence the signaling mechanism, like that reported in normal myotubes and dysgenic myotubes expressing wt-α_{1S}, was Ca^{2+} entry independent [29]. We also expressed fs-α_{1S} in cultured myotubes from two available gene knock-out (KO) mice, lacking the endogenous β1a isoform of the skeletal muscle DHPR [30] and lacking RyR1 [31]. As shown in Fig. 4B, we failed to detect EC coupling in these KO cells transfected with fs-α_{1S}. In summary, the EC coupling expressed by fs-α_{1S} is strictly skeletal-type and requires RyR1 and DHPR β1a.

fs-α_{1S} expresses two complementary protein fragments
The EC coupling recovered by fs-α_{1S} could be due either to the activity of the N-terminal half of α_{1S} alone or to protein-protein complementation between the N-terminal half and a fragment expressing the C-terminal half of α_{1S}. The C-terminal half of α_{1S} could have been translated by the fs-α_{1S} expression vector if the ATG codon (Met701), which is downstream from the TGA termination codon and is in-frame with the wild-type message (Fig 1B) served as open reading frame for translation of the second half of the wt message. Although this would be unusual, the fact that the codon for Met701 is only 25 bases downstream from the termination codon could have substantially increased the possibility of a re-start of the translation of the second half of the message at Met701. This phenomenon has been described in eukaryotic cells and in viral-infected mammalian cells and is known as translation by leaky ribosomal scanning [32,33]. To test this explanation, the presumptive restart condon, Met701, was mutated to Ile701 in the fs-α_{1S} template. If fs-α_{1S} recovered EC coupling by virtue of expressing a single protein fragment, then fs-α_{1S}M701I should also recover EC coupling since the mutation was introduced downstream from the stop codon. Fig. 5 shows that this was not the case. Fs-α_{1S}M701I did not recover Ca^{2+} transients in 9 of 9 tested cells, consistent with leaky ribosomal scanning. As a positive control, we coexpressed fs-α_{1S}M701I and the C-terminus half of α_{1S}, namely $\alpha_{1S}\Delta1$–700, cloned into a separate pSG5 vector. The results in Fig. 5 indicated that $\alpha_{1S}\Delta1$–700 alone was inactive. However, when myotubes were cotransfected with fs-α_{1S}M701I and $\alpha_{1S}\Delta1$–700, each in a separate pSG5 vector, there was a robust recovery of Ca^{2+} transients in 5 of 5 cells. Fig. 6A shows fluorescence vs. voltage relationships for the fs-α_{1S}M701I mutant and for this mutant coexpressed with $\alpha_{1S}\Delta1$–700. The combined expression of the two complementary frag-

ments of α_{1S} resulted in a robust recovery of EC coupling with sigmoidal Ca^{2+} release vs. voltage characteristics. A summary of the maximum fluorescence during the Ca^{2+} transient in response to a depolarization to +90 mV is shown in Fig. 6B. The magnitude of the Ca^{2+} transient expressed by fs-α_{1S}M701I + $\alpha_{1S}\Delta$1–700 was indistinguishable from that of wt-α_{1S} (t-test significance p = 0.671, see figure legend). To confirm expression of the C-terminus half of α_{1S} in cells transfected with fs-α_{1S}, we used the II-III loop polyclonal antibody SKI [34] directed against epitope Ala739-Ile752 which is downstream from Met701. Fig. 6C shows that the II-III loop antibody recognized the C-terminus half when cells were transfected with fs-α_{1S} but not when myotubes were transfected with fs-α_{1S}M701I. The C-terminal protein migrated with a molecular weight of approximately 126 KDa which is consistent with the theoretical molecular weight of 132 KDa. Finally, Fig. 6D shows that fs-α_{1S}M701I was abundantly expressed in myotubes in the absence or presence of the C-terminal fragment. This indicated that the absence of EC coupling observed in myotubes expressing fs-α_{1S}M701I was not due the production of a labile protein. In summary, the recovery of EC coupling by coexpression of two functionally inactive proteins (Fig. 5) taken together with the immunoblots (Fig. 6C) favor the explanation that 1) fs-α_{1S} recovers DHPR function by virtue of expressing two complementary fragments of α_{1S} and 2) the expression of the C-terminal half of α_{1S} by fs-α_{1S} is likely to occur by leaky ribosomal scanning.

Implications for EC coupling in skeletal myotubes

Except for the magnitude, the SR Ca^{2+} release signal expressed by fs-α_{1S} was entirely typical of skeletal myotubes with sigmoidal voltage-dependence, proceeding in the absence of external Ca^{2+} and requiring RyR1. A comparison of the maximum fluorescence (ΔF/Fo max) at +90 mV (Fig. 6B) shows that the signal generated by fs-α_{1S} was significantly smaller than that generated by the control construct (wt-α_{1S} vs. fs-α_{1S} t-test significance p = 0.014) and smaller than that generated by the two coexpressed fragments (fs-α_{1S} vs. fs-α_{1S}M701I + $\alpha_{1S}\Delta$1–700 t-test significance p = 0.013). These observation suggests that the magnitude of the Ca^{2+} release appears to be limited by the low yield of expression of the C-terminal fragment achieved by leaky ribosomal scanning of the second half of the fs-α_{1S} message. To test this explanation further, we coexpressed fs-α_{1S} and the C-terminal half of α_{1S} each in a separate pSG5 vector. We found that fs-α_{1S} and α_1SΔ1–700 together expressed Ca^{2+} transients with a ΔF/Fo max similar to wt-α_{1S} control (not shown). Thus we are certain that the EC coupling expressed by fs-α_{1S} is mechanically similar to control skeletal-type EC coupling but limited in magnitude by a comparatively lower density of functional DHPRs that are assembled in cells expressing fs-α_{1S}. It is conceivable that the functional integrity of the

fragmented α_{1S} protein is maintained in part by the β subunit of the DHPR which spans both halves of the α1 pore subunit by binding to the I-II loop and the C-terminus [35,36]. Consistent with this explanation, we failed to detect EC coupling recovery when fs-α_{1S} was expressed in β1-null myotubes.

Earlier studies in the voltage-gated Na^+ channel had shown that pore function was not compromised when the II-III linker or III-IV linker was cut and the two fragments were coexpressed each in a separate vector [37]. We would thus conclude that in the case of the Ca^{2+} channel, an in-
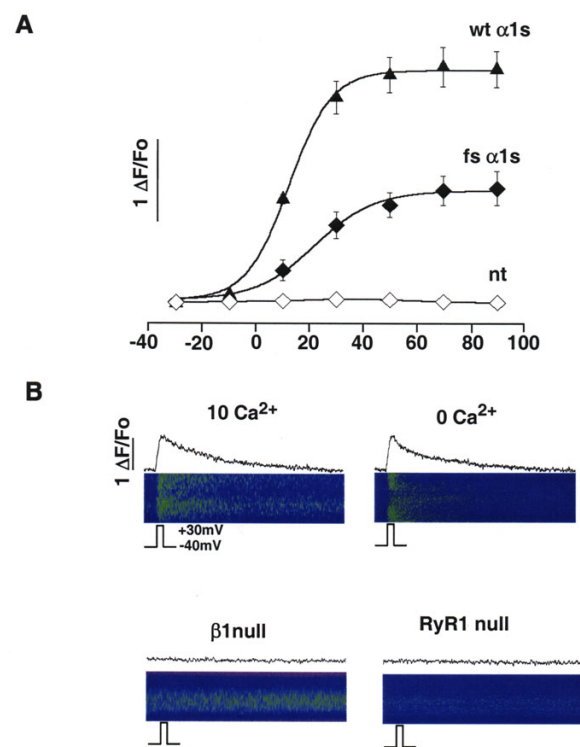
Figure 4
Skeletal-type EC coupling expressed by fs-α_{1S}. A) Voltage-dependence of peak Ca^{2+} for 5 control myotubes expressing wt-α_{1S} and 5 myotubes expressing fs-α_{1S}. Ca_{2+}transients for 15 non-transfected myotubes (NT) are included for reference. The sigmoidal lines are a Boltzmann fit with parameters ΔF/Fo max = 2.9, 1.4 ΔF/Fo; V1/2 = 11.7, 20 mV; k = 8.7, 13.2 mV, for wt-α_{1S} and fs-α_{1S} respectively. B) Line-scans (horizontal dimension is 2.05 seconds) and traces of integrated fluorescence in ΔF/Fo units for depolarizations to +30 mV. Top line-scans are for the same fs-α_{1S} transfected myotube in standard external solution (10 mM $CaCl_2$) and the same solution without added $CaCl_2$ (0 Ca^{2+}). Bottom line-scans show fs-α_{1S} transfected KO myotubes lacking DHPR β1a or lacking RyR1 in standard external solution.
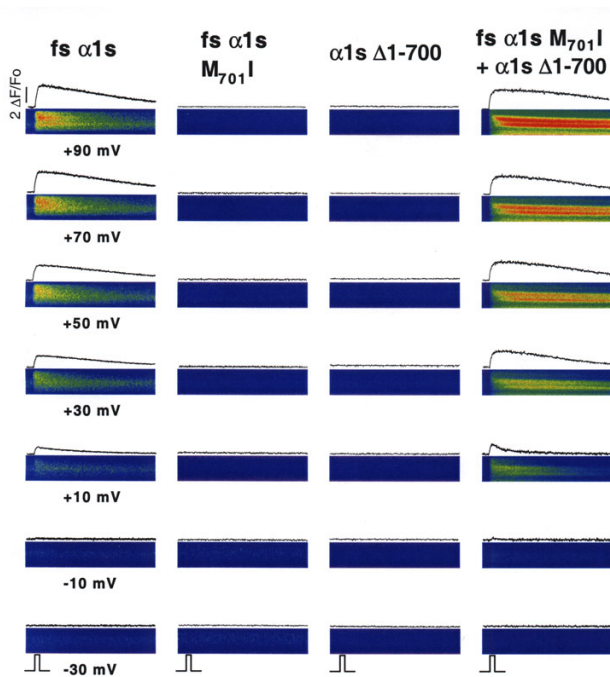
Figure 5
EC coupling generated by two complementary fragments of α_{1S}. Line scans (horizontal dimension is 2.05 seconds) of fluo-4 fluorescence show Ca^{2+} transients in response to the indicated 50-ms depolarization from a holding potential of -40 mV. Trace of integrated fluorescence in $\Delta F/Fo$ units is shown for each line scan. Each set of depolarizations is from a separate dysgenic myotube expressing the α_{1S} construct(s) indicated at the top of each column. A 16-color calibration bar in $\Delta F/Fo$ units is included in Fig. 3 for visual reference.

tact II-III loop is essential for this function since neither fs-α_{1S} nor the combined expression of the two truncated fragments (not shown) was able to rescue Ca^{2+} current. This result is entirely consistent with the identification of the II-III loop as critical for enhancement of L-type Ca^{2+} current expression by the RyR1 [38]. However EC coupling, per se, can clearly proceed with a cut in the II-III loop. This was shown here by the behavior of the fs-α_{1S} construct and elsewhere by expressing the N-terminal half (α_{1S}1–670) and the C-terminal half (α_{1S}701–1873), each with entirely wt sequence and each in a separate expression vector [20]. The fact that Thr671-Leu690 region known as Peptide A [15] is missing in fs-α_{1S} suggests this 20-mer domain is not critical for the conformation change transmitted from the DHPR to the RyR1. To test this further, we generated an in-frame deletion of this region, as originally intended, that showed normal function [20]. Another domain critical for EC coupling is Csk35 downstream from Peptide A (Leu720-Gln765). This region was identified using chimeras of α_{1S} and α_{1C}[16]. Since Csk53 is present in $\alpha_{1S}\Delta$1–700 and was detected by

the II-III loop antibody which is directed against the center portion of Csk53 [34], the participation of this domain in the EC cannot be ruled-out.

In eukaryotic cells, translation starts at the AUG codon nearest to the 5' end of the mRNA, and this initiator site is found by sequential ribosomal scanning in the 5' to 3' direction [32]. However, translation initiation at internal AUGs due to leaky ribosomal scanning has been documented, especially for mRNAs consisting of a short leader ORF upstream from the main ORF. In some cases, reassembly of a new ribosomal initiation complex after the terminator codon of the leader ORF serves to re-initiate translation at the initiator AUG codon for the main ORF, and thus two proteins are generated [39]. In other cases, leaky scanning by the ribosomal initiation complex bypasses the 5'-located leader ORF entirely, and only the "internal" ORF is translated [32]. In the case of fs-α_{1S}, we are not entirely certain which mechanism best applies. A bypass of the ORF at the 5' end of the α_{1S} mRNA in favor of a presumed ORF at Met701 is unlikely because a C-terminal fragment of the size expressed by $\alpha_{1S}\Delta$1–700 has not been detected in skeletal muscle with the SKI antibody [34] or other antibodies [25]. Thus Met701 is not an internal initiation site under normal circumstances. Entry of a new ribosomal complex at Met701 seems a more likely explanation. However, re-initiation after a stop has only been described for cases in which the leader ORF is no longer than 30 codons because initiation factors fall off shortly after recognition of the initiator AUG [32]. In the case of fs-α_{1S}, what can be considered the "leader" ORF encodes for a protein of 671 residues. Hence we are not certain if re-initiation of translation after a stop signal, as currently described in the literature, would apply here. At the same time, it is important to point out that in the present studies, fs-α_{1S} expression is under the control of a viral promoter and that in this hybrid viral-mammalian expression system, the rules pertaining to leaky ribosomal scanning may be different. The mechanism of translation of the fs-α_{1S} clearly deserves closer scrutiny in the future.

Conclusions
The present studies show EC coupling recovery by a frame-shift mutant of α_{1S} due to protein-protein complementation of the N-terminal and C-terminal halves of α_{1S}. The N-terminal half houses repeats I and II with the adjoining cytosolic loop and the C-terminal half houses most of the II-III loop, along with repeats III and IV with the adjoining loop. Protein-protein complementation between the N-terminal and C-terminal fragments produced a DHPR capable of functioning as EC coupling voltage sensor, thus suggesting the presence of at least two functional modules within α_{1S}. Recent evidence suggests that the four internal repeats of the voltage-gated Na^+ channel, which is closely related to the L-type Ca^{2+} channel encod-
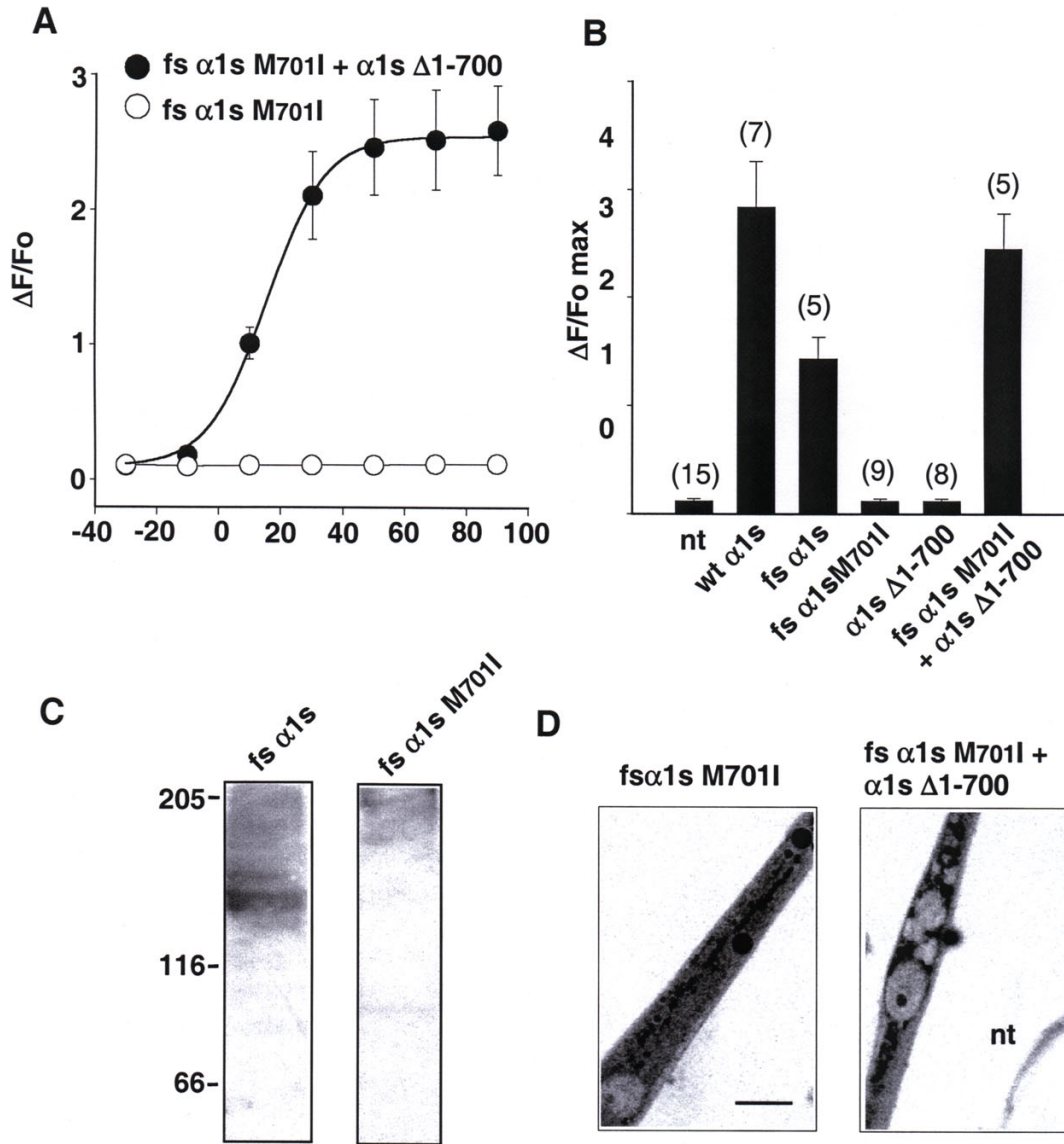
Figure 6

Expression of C-terminal fragment of α_{1S} is essential for EC coupling. A) Voltage dependence of peak Ca^{2+} during the Ca^{2+} transient for dysgenic myotubes transfected with the indicated constructs. The sigmoidal curve is a Boltzmann fit with parameters $\Delta F/Fo$ max = 2.45; $V1/2$ = 15.4 mV; k = 9.3 mV for 5 cells coexpressing fs-α_{1S}M701I + α_{1S}Δ1–700. Absence of response is shown for 9 cells expressing fs-α_{1S}M701I alone. B) $\Delta F/Fo$ max (mean ± SEM) obtained from a depolarization to +90 mV is shown for the indicated number of cells. NT denotes non-transfected dysgenic myotubes. Compared to wt-α_{1S} (control), the statistical significance in unpaired t-Student test was p = 1.6×10^{-6} (non-transfected, NT); 0.014 (fs-α_{1S}); 0.0002 (fs-α_{1S}M701I); 0.0008 (α_{1S}Δ1–700); 0.671 (fs-α_{1S}M701I + α_{1S}Δ1–700). Compared to fs-α_{1S}, the statistical significance was p = 1×10^{-6} (non-transfected, NT); 0.014 (wt-α_{1S}); 0.00019 (fs-α_{1S}M701I); 0.0008 (α_{1S}Δ1–700); 0.013 (fs-α_{1S}M701I + α_{1S}Δ1–700). C) Immunoblots using a polyclonal antibody directed to the II-III loop epitope Ala739-Ile752 [34] in cultures of dysgenic myotubes expressing fs-α_{1S} and fs-α_{1S}M701I. Indicated are 3 of 7 molecular weight markers run in the same gel. D) Confocal images of cells transfected with the CD8 cDNA plus T7-tagged fs-α_{1S}M701I or T7-tagged fs-α_{1S}M701I + untagged α_{1S}Δ1–700. Cells were incubated with CD8 antibody beads, fixed, and stained with T7 primary/ fluorescein-conjugated secondary antibodies Pixel intensity was converted to a 16-level inverted gray scale with high-intensity pixels in black color. NT indicates a non-transfected myotube. CD8 antibody beads have a diameter of 4.5 microns. Calibration bar is 10 microns.

ed by the DHPR, have non-equivalent functional roles because the S4 segments of repeats I and II move much faster than those of repeats III and IV [40]. By analogy, the "fast-moving" module of the DHPR would be represented by the N-terminal fragment and the "slower-moving" module by the C-terminal fragment. Interactions between these two modules are likely to be critical for intramembrane charge movements in the assembled four-repeat channel and for coupling the movement of the S4 gating charges to the opening of the RyR1 channel. Future studies of gating currents in each hemi-Ca^{2+} channel fragment should provide valuable information on how the "fast" and "slow" gating modules interact during EC coupling in skeletal muscle.

The C-terminal fragment was generated by an unusual restart of translation of the fs-α_{1S} message at M701, presumably by leaky ribosomal scanning, and was eliminated by a M701I mutation. Hence, a premature stop codon in the II-III loop upstream of M701 may not necessarily cause a loss of DHPR function because in these cases, function would be recovered by complementation between protein fragments expressed by the same cDNA. From a methodological perspective, leaky scanning could be further used as a means to control protein expression to desired levels, since restart of translation after a premature stop codon is sensitive to the number of nucleotides separating the stop and restart codons [39]. By changing the position of the restart methionine relative to the premature stop codon, it might be possible to significantly change the level of expression of the distal protein fragment and hence functional protein as a whole. Thus, leaky scanning remains as an attractive possibility for boosting or depressing protein levels in a transfected cell.

Materials and Methods
Primary cultures of mouse myotubes
Primary cultures were prepared from hind limbs of day 18 embryos (E18) as described previously [23]. cDNAs of interest and a separate expression vector encoding the T-cell membrane antigen CD8 were subcloned into the mammalian expression vector pSG5 (Stratagene, CA) and were mixed and cotransfected with the polyamine LT-1 (Panvera, WI). Whole-cell recordings and immunostaining were done 3–5 days after transfection. Cotransfected cells were recognized by incubation with CD8 antibody beads (Dynal, Norway). The coincidence of expression of CD8 and a cDNA of interest was >85%.

α_{1S} cDNA constructs
All cDNA constructs were sequenced twice or more using BigDye technology (Perkin Elmer, CA) at a campus facility. For epitope tagging and expression in mammalian cells, the unmodified full-length rabbit α_{1S} cDNA encoding residues 1–1873 (Genebank #M23919 nucleotide co-

ordinates nt 226 to nt 5847) was fused in frame to the first 11 amino acids of the phage T7 gene 10 protein in pSG5 using *AgeI* and *NotI* cloning sites. All constructs were made using the T7 tagged α_{1S} as template in PCR-based strategies, some previously described [20,21]. All primers were HPLC-purified (Operon, CA) and a phosphate was tagged to the 5'-end of the sense primer. Genebank #M23919 nucleotide coordinates are used below to describe primers.

pSG5 wt-α_{1S}
A unique silent *HindIII* site was introduced by PCR at nt 2228 in the full-length α_{1S} template and cloned into the T7-α_{1S} pSG5 vector using *AgeI* and *XhoI* sites. The *HindIII-XhoI* fragment (nt 2228 to nt 2878) encompasing the II-III loop was subcloned into pCR 2.1 TOPO TA (Invitrogen, CA) and this plasmid was further used for PCR reactions.

pSG5 fs-α_{1S}
PCR reactions for deletion of residues 671–690, consisted of 10 nanograms pCR 2.1 TOPO/*HindIII-XhoI* insert, 15 pmoles of each primer, 0.5 mM dNTPs, 1X cloned *Pfu* buffer (Stratagene) and 2.5 U cloned *Pfu* DNA polymerase (Stratagene). The antisense primer was complementary to nt 2202 to nt 2235 and the sense primer was nt 2296 to nt 2326. Amplification was carried out for 30 cycles at 95°C for 45 seconds, 60°C for 2 minutes and 72°C for 2 minutes/kb of plasmid. The PCR reaction was treated with 10 U of *DpnI* (Stratagene) and recircularized with T4 DNA ligase (Stratagene). Once amplified by PCR, the *HindIII-XhoI* digest was ligated into the T7-α_{1S} pSG5 vector using the same restriction sites.

pSG5 fs-α_{1S}M701I
The construct was produced by a two-step PCR reaction using fs α_{1S} as template. Using conditions as above, the sense primer (nt 1932 to nt 1959) was paired with antisense primer 5'TCCAGCTTCTTGGCGATCACAGACTTCTCC3' carrying the point mutation. In a seperate reaction, sense primer 5'GGAGAAGTCTGTGATCGCCAAGAAGCTGGA3' was paired with antisense primer (nt 3100 to nt 3081). The two PCR products were diluted 1:500 in ddH$_2$O and then hybridized to each other for 2 minutes at 95°C, 1 minute at 43°C and 1 minute at 72°C for 4 cycles. 15 pmol of nt 1932 to nt 1959 primer and 15 pmol of nt 3100 to 3081 primer were added and further cycled for 4 minutes at 95°C, then 30X of 2 minutes at 95°C, 1 minute at 60°C, 1 minute at 72°C and finally 10 minutes at 72°C. The PCR product was then cloned into the fs α_{1S} construct using *HindIII* and *XhoI* sites.

pSG5 a$_{1S}$Δ1–700
The construct was produced by cutting pSG5 fs α_{1S} with *AgeI* and *HindIII* enzymes and filling-in the overhangs

with klenow fragments. The plasmid was religated using DNA T4 ligase.

Whole-cell voltage-clamp

Whole-cell recordings were performed as described previously [22] using an Axopatch 200B amplifier (Axon Instruments, Foster City, CA). All experiments were performed at room temperature. Patch pipettes had a resistance of 1–2 MΩ . The external solution was (in mM) 130 TEA-Methanesulfonate, 10 CaCl$_2$, 1 MgCl$_2$, 10 HEPES-TEA(OH), pH 7.4. The pipette solution was (in mM) 140 Cs-aspartate, 5 MgCl$_2$, 0.1 EGTA (for Ca^{2+} transients) or 5 EGTA (for Ca^{2+} current), 10 MOPS-CsOH, pH 7.2. The voltage dependence of peak intracellular Ca^{2+} (ΔF/Fo) was fitted according to a Boltzmann distribution (Eqn. 1) A = A$_{max}$/(1+exp(-(V-V$_{1/2}$)/k)). A$_{max}$ is ΔF/Fo$_{max}$; V$_{1/2}$ is the potential at which A = A$_{max}$/2; and k is the slope factor. ΔF/Fo=(F-Fo)/Fo where F is the fluorescence during a Ca^{2+} transient and Fo is the resting fluorescence of the cell immediately before the stimulation.

Confocal fluorescence microscopy

Line-scans were performed as described [26] in cells loaded with 4 mM fluo-3 AM (fluo-3 acetoxymethyl ester, Molecular Probes, OR) for ∼30 minutes at room temperature. Cells were viewed with an inverted Olympus microscope with a 20X objective (N.A. 0.4) and a Fluoview confocal attachment (Olympus, NY). Excitation light was provided by a 5 mW Argon laser attenuated to 20% with neutral density filters. For immunofluorescence, confocal images had a dimension of 1024 by 1024 pixels (0.35 microns/pixel) and were obtained with a 40X oil-immersion objective (N.A. 1.3).

Immunostaining

Cells were fixed and processed for immunofluorescence as described [4,20]. The N-terminal fragment expressed by fs-α_{1S} or wt-α_{1S} was identified with a mouse monoclonal antibody against a T7 epitope fused to the N-terminus of α_{1S}. The anti-T7 antibody (Novagen, WI) was used at a dilution of 1:1000. Secondary antibodies were a fluorescein-conjugated goat anti mouse IgG (Boehringer Mannheim, IN) used at a dilution of 1:1000 and a fluorescein-conjugated donkey anti-rabbit IgG (Chemicon, CA) used at a dilution of 1:1000.

Western blots

The C-terminal fragment was identified with SKI, a rabbit polyclonal antibody against the II-III loop of α_{1S} (Ala739-Ile752) previously characterized [34]. Cells were scrapped from tissue cultures dishes with cold PBS plus protease inhibitors and spun in a cold table-top centrifuge. Cells were homogenized in a glass-teflon homogenizer in a minimal volume of PBS and diluted 1:1 (vol:vol) with SDS-gel loading buffer composed 100 mM Tris-Cl (pH 6.8), 200 mM dithiothreitol, 4% SDS, 0.2% bromophenol blue and 20% glycerol. Samples were incubated at 100°C for 20 minutes. Approximately 10 mg of total protein was applied to a 5–15% SDS polyacrylamide gel and electrophoresed for 2 hours at 40 mA. Proteins were transferred to PVDF membranes and analyzed with either anti-T7 or SKI antibodies and the appropriate secondary antibodies. The subunits were visualized using SuperSignal ECL reagent (Pierce, Rockford, IL). The images were captured on a Chemi-Imager (Alpha Innotech, San Leandro, CA) set to a level just below saturation.

Abbreviations

DMSO (dimethyl sulfoxide); EGTA (ethylene glycol bis-α minoethylether tetraacetic acid); HEPES (2-hydroxylethyl piperazine 2-ethane sulfonic acid); MOPS (3N-Morpholino-propane sulfonic acid); PVDF (polyvinylidene difluoride); TTX (tetrodotoxin); TEA (tetraethylamonium); ORF (origin of replication).

Acknowledgements

References

1. Perez-Reyes E, Schneider T: **Calcium channels: Structure, Function, and Classification.** *Drug Dev Res* 1994, **33**:295-318
2. Catterall WA: **Structure and function of voltage-gated ion channels.** *Annu Rev Biochem* 1995, **64**:493-531
3. Birnbaumer L, Qin N, Olcese R, Tareilus E, Platano D, Costantin D, Stefani E: **Structures and functions of calcium channel β subunits.** *J Bioenereg Biomemb* 1998, **30**:357-375
4. Beurg M, Ahern CA, Vallejo P, Conklin MW, Powers PA, Gregg RG, Coronado R: **Involvement of the carboxy-terminus region of the dihydropyridine receptor β_{1a} subunit in excitation-contraction coupling of skeletal muscle.** *Biophys J* 1999, **77**:2953-296
5. Gurnett CA, De Waard M, Campbell KP: **Dual function of the voltage-dependent Ca^{2+} channel α2-δ subunit in current stimulation and subunit interaction.** *Neuron* 1996, **16**:431-440
6. Jay SD, Ellis SB, McCue AF, Williams ME, Vedvick TS, Harpold MM, Campbell KP: **Primary structure of the γ subunit of the L-type calcium channel from rabbit skeletal muscle.** *Science* 1990, **248**:490-492
7. Ahern CA, Powers PA, Biddlecome GH, Roethe L, Vallejo P, Mortenson L, Strube C, Campbell KP, Coronado R, Gregg RG: **Modulation of L-type Ca^{2+} current but not activation of Ca^{2+} release by the γ_l subunit of the dihydropyridine receptor of skeletal muscle.** *BiomedCentral Physiol* 2001, **1**:8 [www.biomedcentral.com/1472-6793/1/8]
8. Block BA, Imagawa T, Campbell KP, Franzini-αrmstrong CA: **Structural evidence for direct interaction between the molecular components of the transverse tubule/sarcoplasmic reticulum junction in skeletal muscle.** *J Cell Biol* 1988, **107**:2587-2600
9. Tanabe T, Beam KG, Adams BA, Niidome T, Numa S: **Regions of the skeletal muscle dihydropyridine receptor critical for excitation-contraction coupling.** *Nature* 1990, **346**:567-569
10. Adams BA, Tanabe T, Mikami A, Numa S, Beam KG: **Intramembrane charge movement restored in dysgenic skeletal muscle by injection of dihydropyridine receptor cDNAs.** *Nature* 1990, **346**:569-572
11. Garcia J, Beam KG: **Relationship of calcium transients to calcium currents and charge movements in myotubes expressing skeletal and cardiac dihydropyridine receptors.** *J Gen Physiol* 1984, **104**:1113-1128

12. McPherson PS, Campbell KP: **The ryanodine receptor/Ca^{2+} release channel.** *J Biol Chem* 1993, **268**:13765-13768
13. Sutko JJ, Airey JA: **Ryanodine receptor Ca^{2+} release channels: Does diversity in form equal diversity in function?** *Physiol Revs* 1996, **76**:1027-1071
14. Lu X, Xu L, Meissner G: **Activation of the skeletal muscle calcium release channel by a cytoplasmic loop of the dihydropyridine receptor.** *J Biol Chem* 1994, **269**:6511-6516
15. El-Hayek R, Antoniu B, Wang J, Hamilton SL, Ikemoto N: **Identification of the calcium release-trigger and blocking regions of the II-III loop of the skeletal muscle dihydropyridine receptor.** *J Biol Chem* 1995, **270**:22116-22118
16. Nakai J, Tanabe T, Konno T, Adams B, Beam KG: **Localization in the II-III loop of the dihydropyridine receptor of a sequence critical for excitation-contraction coupling.** *J Biol Chem* 1998, **273**:24983-24986
17. Leong P, MacLennan DH: **The cytoplasmic loops between domains II and III and domains III and IV in the skeletal muscle dihydropyridine receptor bind to a contiguous site in the skeletal muscle ryanodine receptors.** *J Biol Chem* 1998, **273**:29958-29964
18. Saiki Y, El-Hayek R, Ikemoto N: **Involvement of the Glu724-Pro760 region of the dihydropyridine receptor II-III loop in skeletal muscle excitation-contraction coupling.** *J Biol Chem* 1999, **274**:7825-7832
19. Wilkens CM, Kasielke N, Flucher BE, Beam KG, Grabner M: **Excitation-contraction coupling is unaffected by drastic alteration of the sequence surrounding residues L-720-L764 of the α_{1S} II-III loop.** *Proc Natl Acad Sci USA* 2001, **98**:5892-5897
20. Ahern CA, Arikkath J, Vallejo P, Gurnett CA, Powers PA, Campbell KP, Coronado R: **Intramembrane charge movements and excitation-contraction coupling expressed by two-domain fragments of the Ca^{2+} channel.** *Proc Natl Acad Sci USA* 2001, **98**:6935-6940
21. Ahern CA, Bhattacharya D, Mortenson L, Coronado R: **A component of excitation-contraction coupling triggered in the absence of the T671-L690 and L720-Q765 regions of the II-III loop of the dihydropyridine receptor α_{1S} pore subunit.** *Biophys J* 2001, **81**:3294-3307
22. Strube C, Beurg M, Powers PA, Gregg RG, Coronado R: **Reduced Ca^{2+} current, charge movement and absence of Ca^{2+} transients in skeletal muscle deficient in dihydropyridine receptor β_1 subunit.** *Biophys J* 1996, **71**:2531-2543
23. Beurg M, Sukhareva M, Strube C, Powers PA, Gregg RG, Coronado R: **Recovery of Ca^{2+} current, charge movements, and Ca^{2+} transients in myotubes deficient in dihydropyridine receptor β_1 subunit transfected with β_1 cDNA.** *Biophys J* 1997, **73**:807-818
24. Beurg M, Sukhareva M, Ahern CA, Conklin MW, Powell JA, Powers PA, Gregg RG, Coronado R: **Differential control of skeletal muscle Ca^{2+} current and excitation-contraction coupling by the dihydropyridine receptor β subunit.** *Biophys J* 1999, **76**:1744-1756
25. Leung AT, Imagawa T, Campbell KP: **Structural characterization of the 1,4 dihydropyridine receptor of the voltage-dependent Ca^{2+} channel from rabbit skeletal muscle: evidence for two distinct high molecular weight subunits.** *J. Biol Chem* 1987, **262**:7943-7946
26. Conklin MW, Ahern CA, Vallejo P, Sorrentino V, Takeshima H, Coronado R: **Comparison of Ca^{2+} sparks produced independently by two ryanodine receptor isoforms (type-1 or type-3).** *Biophys J* 2000, **78**:1777-1785
27. Adams BA, Beam KG: **A novel calcium current in dysgenic skeletal muscle.** *J Gen Physiol* 1990, **94**:429-444
28. Strube C, Beurg M, Sukhareva M, Ahern C, Powell JA, Powers PA, Gregg RG, Coronado R: **Molecular origin of the Ca^{2+} current of skeletal muscle myotubes selectively deficient in dihydropyridine receptor β_1 subunit.** *Biophys J* 1998, **75**:207-217
29. Dirksen RT, Beam KG: **Role of calcium permeation in dihydropyridine receptor function. Insights into channel gating and excitation-contraction coupling.** *J Gen Physiol* 1999, **114**:393-403
30. Gregg RG, Messing A, Strube C, Beurg M, Moss R, Behan M, Sukhareva M, Haynes S, Powell JA, Coronado R, Powers PA: **Absence of the β subunit (*cchb1*) of the skeletal muscle dihydropyridine receptor alters expression of the α_1 subunit and eliminates excitation-contraction coupling.** *Proc Natl Acad Sci USA* 1996, **93**:13961-13966
31. Takeshima H, Iino M, Takekura H, Nishi M, Kuno J, Minowa O, Takano H, Noda T: **Excitation-contraction coupling and muscular degeneration in mice lacking functional skeletal muscle ryanodine receptor gene.** *Nature* 1994, **369**:556-559
32. Kozak M: **Initiation of translation in prokaryotes and eukaryotes.** *Gene* 1999, **234**:187-208
33. Liu Q, Hobom G: **Evidence for translation of VP3 of avian polyomavirus BFDV by leaky ribosomal scanning.** *Arch Virol* 2000, **145**:407-416
34. Brawley RM, Hosey MM: **Identification of two distinct proteins that are immunologically related to the α_1 subunit of the skeletal muscle dihydropyridine sensitive calcium channel.** *J Biol Chem* 1992, **267**:18218-18223
35. De Waard M, Pragnell M, Campbell KP: **Ca^{2+} channel regulation by a conserved β subunit domain.** *Neuron* 1994, **13**:495-503
36. Tareilus E, Roux M, Qin N, Olcese R, Zhou J, Stefani E, Birnbaumer L: **A *Xenopus* oocyte β subunit: Evidence for a role in the assembly/expression of voltage-gated calcium channels that is separate from its role as a regulatory subunit.** *Proc Natl Acad Sci USA* 1997, **94**:1703-1708
37. Stühmer W, Conti F, Suzuki H, Wang X, Noda M, Yahagi N, Kubo H, Numa S: **Structural parts involved in activation and inactivation of sodium channels.** *Nature* 1989, **339**:597-603
38. Grabner M, Dirksen DT, Beam KG: **The II-III loop of the skeletal muscle dihydropyridine receptor is responsible for bi-directional coupling with the ryanodine receptor.** *J Biol Chem* 1999, **274**:21913-21919
39. Kozak M: **Analysis of vertebrate mRNA sequences: intimations of translation control.** *J Cell Biol* 1991, **115**:887-903
40. Bezanilla F: **The voltage sensor in voltage-dependent ion channels.** *Physiol Revs* 2000, **80**:555-592